Desalination and Water Treatment
www.deswater.com

doi: 10.5004/dwt.2018.22156

119 (2018) 9–15
July

Comparison of hydrodynamics by backwashing and channel washing within hollow fiber membrane module using computational fluid dynamics

Changkyoo Choi, Chulmin Lee, In S. Kim*

Global Desalination Research Center (GDRC), School of Earth Sciences and Environmental Engineering, Gwangju Institute of Science and Technology (GIST), 123 Cheomdangwagi-ro, Buk-gu, Gwangju, 61005, Korea, Tel. +82-62-715-2436; Fax: 82-62-715-2434; email: iskim@gist.ac.kr (I.S. Kim)

Received 19 December 2017; Accepted 15 February 2018

ABSTRACT

This paper investigated the streamline, velocity vector, and velocity and pressure profiles of fluid to find out the potential of cleaning by backwashing and channel washing at membrane pores and inner surface of inside-out filtration pressurized hollow fiber membrane using computational fluid dynamics simulation. The results of streamline in the module and membrane showed that foulants accumulated on the membrane inner surface is difficult to completely eliminate by backwashing, however, channel washing successfully performed due to the strong velocity streamline. Channel washing showed more than 42 times of an average velocity at membrane inner surface and pores compared with backwashing. The applied pressure on module and membrane in channel washing was much lower than that of backwashing because most injected fluid flows directly from module inlet to outlet without penetrating membrane. The velocity and pressure profiles at pores and inner surface of membrane fiber by backwashing and channel washing showed that the velocity within the membrane pores at channel washing maintained at much higher range and the pressure on the membrane at channel washing was a lot of fluctuation due to better filtration performance.

Keywords: Backwashing; Channel washing; Hollow fiber membrane module; Computational fluid dynamics

1. Introduction

Hollow fiber membrane (HFM) has been widely used in water treatment industries [1–3]. The shape of HFM is cylindrical and are commonly made with bundles within hollow fiber membrane module (HFMM) [4,5]. And, some geometrical parameters are important to determine the performance of HFMM, for example, the length and diameter of membrane fiber and module size [6].

In general, microfiltration (MF) and ultrafiltration (UF) have been manufactured with pressurized membrane modules and applied across various fields, including wastewater treatment and desalination industries. MF/UF membrane module designs employ a hollow fiber configuration, with advantages of its low cost and high surface area unit per volume. For this reason, MF/UF with pressurized HFMM is economically attractive and effective in a field application [7,8].

A source of poor performance of the HFMM has been known to be uneven flows within a module [9]. The uneven flows create regions with extremely low or high local flux, and it is detrimental to the performance of the HFMM for a few reasons: low productivity, shorter operation cycle, and life of the module [10].

In parallel with broad experimental studies to find out the hydrodynamics in HFMM, computational fluid dynamics (CFD) modeling has been employed to analyze fluid behaviors within a membrane module [11,12]. With the visualization of the fluid velocity, pressure and temperature profiles at whole module and specific points, CFD can identify the fundamental mass transfer with fluid hydrodynamics [13]. CFD modeling has also been adopted

* Corresponding author.

Presented at the 10th International Desalination Workshop (IDW 2017), November 22–25, 2017, Busan, Korea.

to simulate fluid dynamic behavior in membrane contactors to predict shell-side flow and mass transfer by simulating individual hollow fiber using the Navier–Stokes equations. Yang et al. [13] simulated using CFD to explore the potential of micro-structured hollow fiber designs to improve the performance in a direct-contact membrane distillation process. As a result, it proved that a gear-shaped fiber design showed an improvement of average temperature polarization coefficient and mass flux. Zhuang et al. [10] investigated the flux distribution in dead-end outside-in HFMM using CFD simulation and verified when compared with experimental results, and it proved that the shell void fraction used in the simulation is 0.8 and the experimental results are in good agreement with that of CFD simulation.

Backwashing is a crucial process in membrane filtration, which maintained the filtration performance of the membrane. Fluid flows through the membrane pores against the flow direction (inside-out or outside-in) of the filtration and washes the attached foulants away on membrane surface and within membrane pores formed during filtration process. Under the same pressure values on membrane module, the faster the fluid flows, the better the fouling layer removal at backwashing [14]. Inside-out type module with hollow fibers is practically not possible to generate the turbulence that is important to remove cake layer on membrane surface, due to the small inner diameter of membrane fiber and the low water velocity comparing with out-to-in [15]. Guo et al. [16] analyzed the variation of the fouling layer on the membrane surface during backwashing, and the impact of shear stress caused by air scouring process was investigated through CFD and verified by experimental studies. It revealed that the results of CFD simulation were in accordance with the experimental results in terms of cleaning efficiency during backwashing.

The purpose of this paper is to simulate the streamline, velocity vector, and profiles of velocity and pressure of fluid to find out the potential of cleaning in order to suggest the newly designed module, which can wash the inner side of membrane hollow fiber, of inside-out filtration mode using CFD technique. To indirectly investigate a washing efficiency, fluid velocity and pressure values were compared at module, membrane surface, and membrane inside.

2. Methods

2.1. Governing equations

Interpretation of fluid behavior is significantly difficult, even if the prediction of fluid flow on module configuration is not impossible. CFD is a strong tool that has successfully been used to analyze the fluid flow behavior. In this study, to simulate the fluid hydrodynamics, ANSYS CFX (version 18.0) was employed. CFX is one of high-performance CFD software tools with an outstanding accuracy in its hydraulic analysis of membrane modules [17]. The governing equation of ANSYS CFX is the Navier–Stokes equation, which well describes mass transport processes. This fluid is assumed to be Newtonian when the flow is in a steady state [18]. The convective acceleration term can describe the effect of a fluid flow on space, and modified Navier–Stokes equation at x direction is as follows [14].

$$\rho\left(v_x\frac{\partial v_x}{\partial x}+v_y\frac{v_x}{\partial y}+v_z\frac{\partial v_x}{\partial z}\right)+\frac{\partial p}{\partial x}-g_x=\eta_\varepsilon\nabla^2 v_x-\frac{\eta}{K_{\text{porous}}}v_x \quad (1)$$

A wide range of turbulent eddy size characteristics is included in a turbulent flow. The Reynolds-averaged Navier–Stokes (RANS) simulation, which is the solution of time-averaged equations and is the most widely used approach for estimating industrial flows, is applied with the averaging procedure to the Navier–Stokes momentum as Eq. (2) [19]. The Reynolds stresses, R_{ij}, are additional unknowns introduced by the averaging procedure, and they have modeled to approach the system of governing equations of Eq. (3).

$$\rho\left(\frac{\partial\overline{u}_i}{\partial t}+u_k\frac{\partial\overline{u}_i}{\partial x_k}\right)=-\frac{\partial\overline{p}}{\partial x_i}+\frac{\partial}{\partial x_j}\left(\mu\frac{\partial\overline{u}_i}{\partial x_j}\right)+\frac{\partial R_{ij}}{\partial x_j} \quad (2)$$

$$R_{ij}=-\rho\overline{u_i u_j} \quad (3)$$

where u_i and x_i are the velocity and distance in i direction, u_j and x_j are the velocity and distance in j direction, u_k and x_k are the velocity and distance in k direction, p is the average pressure, ρ is the kinematic viscosity, μ is the dynamic viscosity, and R_{ij} is the Reynolds stress.

2.2. Module configuration

The membrane module with one membrane fiber (porous domain) used in this study was employed, and the detailed schematic diagram is shown in Fig. 1. Two inflow pipes located at both edge side on the outside of module designated as inlet with the pressure of 2 bar, and the simulation was carried out that the cleaning water passes from outside to the inside of a membrane fiber and discharges to both ends of the membrane fiber. On contrary, in channel washing mode, the cleaning water with a pressure of 2 bar is injected at one end of a membrane fiber, and it passes from outside to inside of a membrane fiber and discharges to the pipe located at bottom side of a module. The remained cleaning water, which is not passing through membrane, passes to other end of a membrane fiber after washing inner surface of membrane. The detailed specifications of the module and membrane are shown in Table 1.

2.3. Boundary conditions

Simulations in this study were conducted using 3D flows. In the CFD, the boundary condition can be set based on the flow rate, pressure, and velocity. Main boundary condition in this study is set as a pressure in inlet. In general, the inlet pressure for backwashing in MF/UF is in the range of 3–7 bars, and an error occurred under CFD simulation at this pressure range. Hence, the inlet pressure was set to 2 bar, which is the highest pressure within the range of no error. Also, it was considered that the difference of inlet flow rate in backwashing and channel washing was due to the difference of an effective inlet area under same pressure. The fluid flow was set as turbulent mode, because the Reynolds number

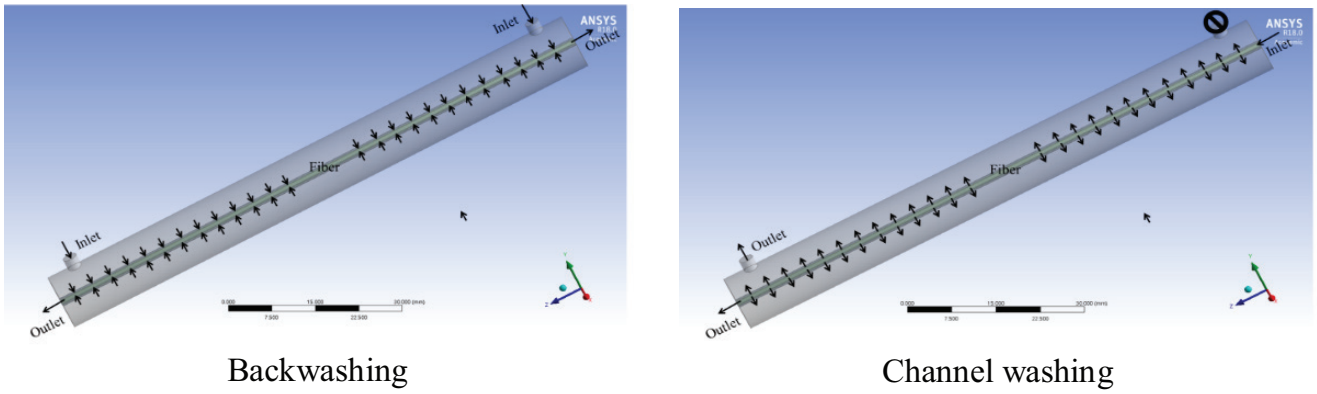

Fig. 1. The module configuration for backwashing and channel washing.

Table 1
Specification of module and membrane

	Backwashing	Channel washing
Module length (mm)	100	
Module diameter (mm)	10	
Fiber porosity (%)	80	
Fiber length (mm)	100	
Fiber OD/ID (mm)	1.55/0.9	
Inlet area (mm^2)	9.71	0.63
Outlet area (mm^2)	1.26	5.49

OD: outer diameter, ID: inner diameter.

Table 2
Boundary conditions for CFD simulations

	Backwashing	Channel washing
Dimension	3D	
Flow mode	Turbulent	
Inlet flow rate (L/s)	0.02 (at 2 bar)	0.11 (at 2 bar)
Fluid temperature (°C)	20	

was much larger than 2,600. The wall boundary conditions were applied under non-slip conditions. The detailed boundary conditions are shown in Table 2.

3. Results and discussion

3.1. Streamline and velocity vector on module

From the results of streamline at the module and membrane in Fig. 2, in the backwashing (Fig. 2(a)), the cleaning water from inlet was filled within the module, however, most fluid did not flow at the center of the membrane inside as Fig. 2(c) and went out to both sides of membrane fiber. It was found that the washing of the whole membrane inside was not performed because the fluid flow was concentrated at both sides of membrane which was close to outlet. On the other hand, in channel washing (Fig. 2(b)), the cleaning water from the inlet flowed through the whole membrane inside, and it went out to outlet in membrane fiber. The fluid after passing through the membrane quickly went out to outlet located in lower side of module. It proved that channel washing achieved not only membrane pores washing but also membrane inside washing.

In streamline within membrane by backwashing (Fig. 2(c)), the fluid seems to flow throughout the membrane inside, but the velocity streamline is very high at both ends and relatively weak at the center. From the streamline in a membrane fiber by channel washing (Fig. 2(d)), the fluid also flows throughout the membrane inside, however, velocity is higher at the vicinity of inlet and relatively weak from center to end of membrane fiber, because much cleaning water passes through the membrane.

As above results, considering that most of the foulants accumulate in the membrane inner surface at an inside-out filtration, it estimates that foulants at the center part of the membrane inside is difficult to completely eliminate by backwashing, however, foulants removal efficiency by channel washing is relatively increased due to the strong velocity streamline.

In the velocity vector in Fig. 3, most cleaning water from inlet passes through both edges of membrane outer surface in module, and goes out to outlet at both ends of membrane inside by backwashing (Fig. 3(a)). From the velocity vector of membrane inside (Fig. 3(c)), a strong fluid flow is at both ends rather than the center of the membrane inside. In the velocity vector at a channel washing (Fig. 3(b)), the cleaning water at the inlet part was strongly permeated from inside to outside of membrane fiber, simultaneously, it continuously was permeated as the fluid moved to the outlet of membrane inside.

From these results, channel washing can be more efficient than backwashing in order to remove foulants accumulated at the membrane inside at the module of inside-out filtration.

3.2. Velocity and pressure on module

Fig. 4 shows the average velocity and pressure values of a fluid flow on module and membrane at backwashing and channel washing. The fluid from inlet flowed into membrane outer surface, after then, through membrane pores and membrane inner surface, it outflowed to outlet at backwashing. In case of channel washing, the fluid from inlet flowed into membrane inner surface, then, through membrane pores and membrane outer surface, it outflowed to outlet.

The velocity and pressure values across the module were 1.38 m/s and 197 kPa at backwashing and 21.6 m/s and

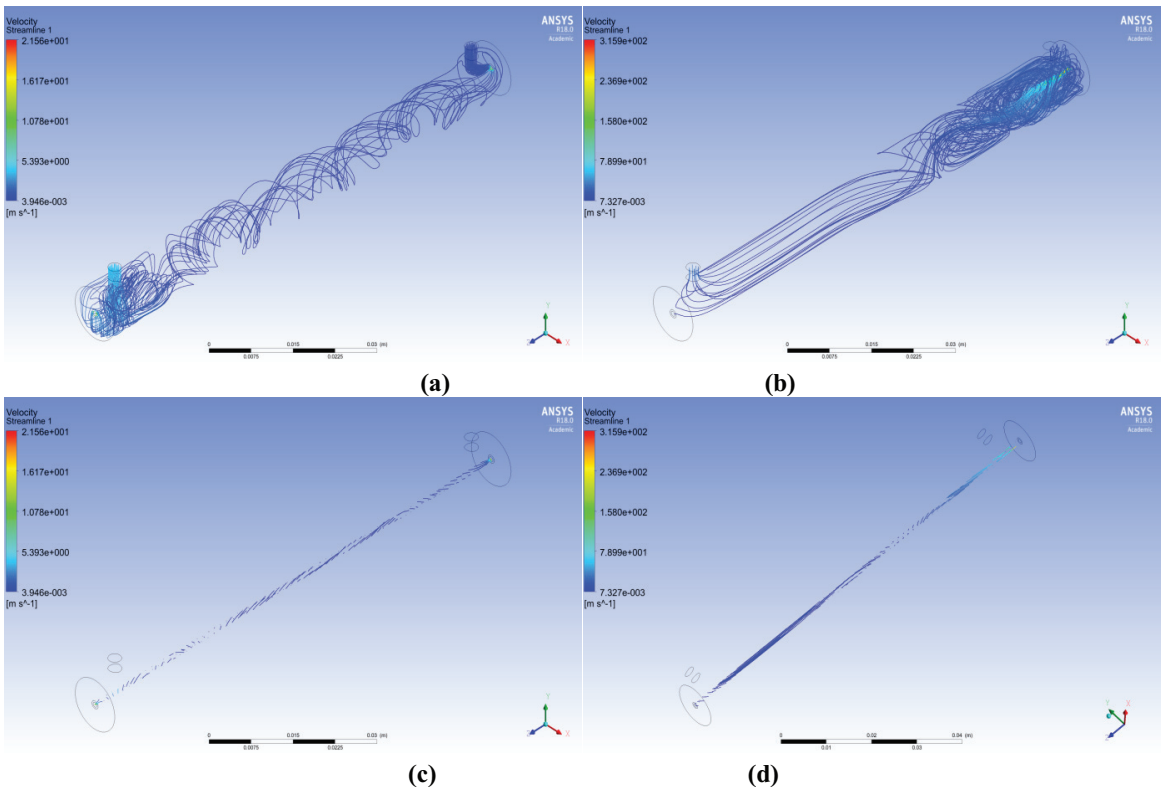

Fig. 2. Streamlines (a) at module when backwashing, (b) at module when channel washing, (c) at membrane when backwashing, and (d) at membrane when channel washing.

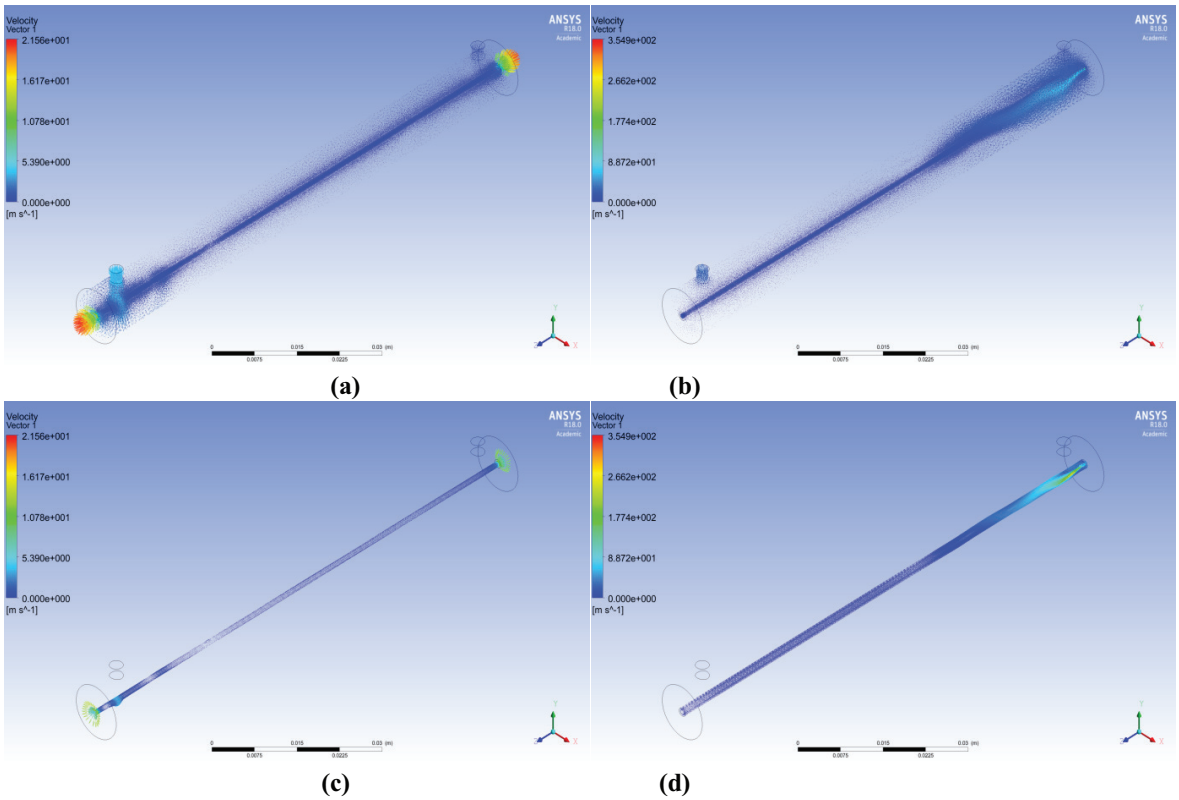

Fig. 3. Velocity vector (a) at module when backwashing, (b) at module when channel washing, (c) at membrane when backwashing, and (d) at membrane when channel washing.

52 kPa at channel washing, respectively. The channel washing showed a stronger flow rate about 15.6 times than backwashing throughout the module.

The high pressure was maintained from inlet to the membrane inner surface because the fluid did not smoothly pass through the membrane, and the cleaning water was stagnated in the module. On the contrary, in channel washing, low pressure was maintained at the inlet part because some fluid passed from the inner surface to the outside of membrane, and the rest went out to the outlet at a membrane inside. As seen at each part, the velocity values of channel washing were 86 times higher in the inlet, 27 times in the membrane pores, and 56 times in the membrane inner surface than those of backwashing, respectively. It proved that the foulants attached to the pores and inner surface of membrane could be removed by fluid flow with a high velocity.

As shown in the above results, channel washing showed more than 15 times higher velocity than backwashing, especially, it was more than 42 times of an average velocity at membrane inner surface and pores showing the high efficiency of membrane cleaning.

3.3. Velocity and pressure on membrane

3.3.1. Velocity on membrane

Fig. 5 showed the results of velocity profile at pores and inner surface of membrane fiber by backwashing and channel washing, then the x-axis is cell counts which is mesh number on the pores and inner surface of membrane fiber. The velocity values of membrane pores at backwashing were the maximum of 12.110 m/s and minimum of 0.048 m/s, showing an average of 0.332 m/s, and those at channel washing were the maximum of 225.034 m/s and the minimum of 1.113 m/s which was an average of 8.948 m/s. It proved that the velocity distribution at channel washing showed a much higher range within the membrane pores.

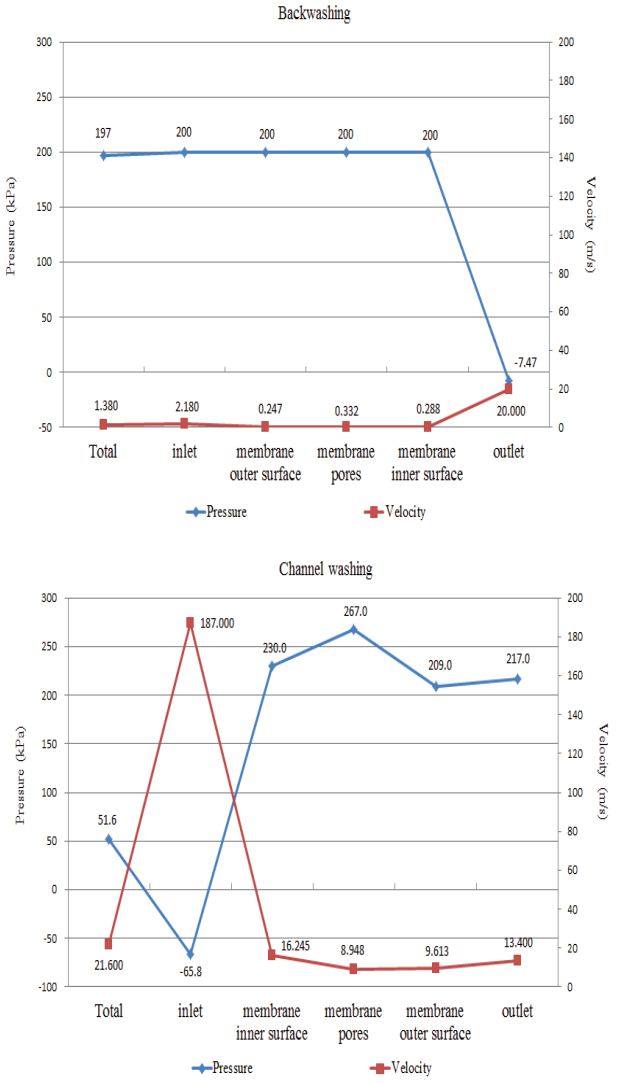

Fig. 4. Average velocity and pressure values at backwashing and channel washing on module and membrane.

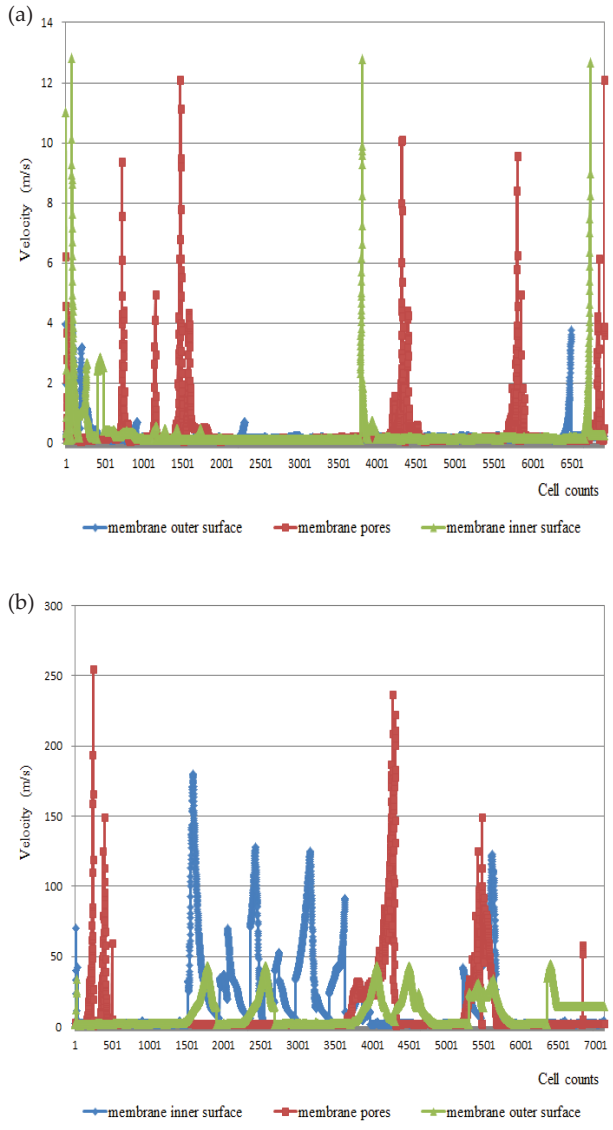

Fig. 5. Velocity profile at (a) backwashing on membrane and (b) channel washing on membrane.

The velocity values of membrane inner surface at backwashing were the maximum of 12.842 m/s and the minimum of 0.084 m/s, showing an average of 0.284 m/s, and those at channel washing were the maximum of 180.006 m/s and the minimum of 1.337 m/s which was an average of 16.245 m/s. It proved that membrane fouling at channel washing could be more reduced by high flow velocity on the membrane inner surface where most foulants were accumulated.

Also, in the velocity profile at the membrane inner surface by backwashing, the relatively high velocity values were observed at upper, middle, and lower parts, however, the frequency of the high velocity in channel washing was much more at membrane inner surface. This also showed a high removal potential of foulants accumulated on the membrane inner surface.

3.3.2. *Pressure on membrane*

In the pressure profile on the membrane of Fig. 6, the pressure values of membrane outer surface at backwashing were the maximum of 200 kPa and minimum of 194 kPa, showing an average of 200 kPa, and those of membrane inner surface were the maximum of 201 kPa and the minimum of 104 kPa which was an average of 200 kPa, then the average pressure difference from outer surface to inner surface on membrane fiber was 0.207 kPa. The pressure values of membrane inner surface at channel washing were the maximum of 311 kPa and minimum of –514 kPa, showing an average of 230 kPa, and those of membrane outer surface were the maximum of 311 kPa and the minimum of –143 kPa which was an average of 209 kPa, then the average pressure difference from inner surface to outer surface on membrane fiber was 20.5 kPa. The pressure at backwashing was maintained at almost constant on membrane, and it is due that the membrane filtration of the fluid is not successfully performed. On the contrary, the pressure values at channel washing showed a lot of fluctuation on the membrane, and pressure fluctuation meant that more fluid passed through membrane surface, which indicated that membrane filtration is better performed under high fluid velocity, and then the pressure change on membrane surface and pores is large.

As shown in the above results, it proved that channel washing with high velocity and consequently low pressure on pores and inner surface of the membrane is able to better remove the foulants attached to membrane inside than backwashing.

4. Conclusions

This paper investigated the streamline, velocity vector, and velocity and pressure profiles of fluid to find out the potential of cleaning by backwashing and channel washing at membrane pores and inner surface of inside-out filtration pressurized HFM using CFD simulation.

- From the results of streamline at the module and membrane, it indirectly found that the foulants, which accumulated on the membrane inner surface in an inside-out filtration mode, are difficult to completely eliminate by backwashing, however, foulants removal by channel washing may be successfully performed due to the strong velocity streamline.
- In the average velocity and pressure values of a fluid flow on module and membrane at backwashing and channel washing, channel washing showed more than 42 times of an average velocity at membrane inner surface and pores. The pressure at channel washing was lower than backwashing on module and membrane because most fluid passed from the inlet to the outlet.
- In the velocity and pressure profiles at pores and inner surface of membrane fiber by backwashing and channel washing, the range of velocity at channel washing was a much higher within the membrane pores. The pressure at backwashing was maintained highly on membrane due to the unsuccessful filtration, however, the pressure at channel washing showed a lot of fluctuation on the membrane due to better filtration performance under high fluid velocity and consequently low pressure.

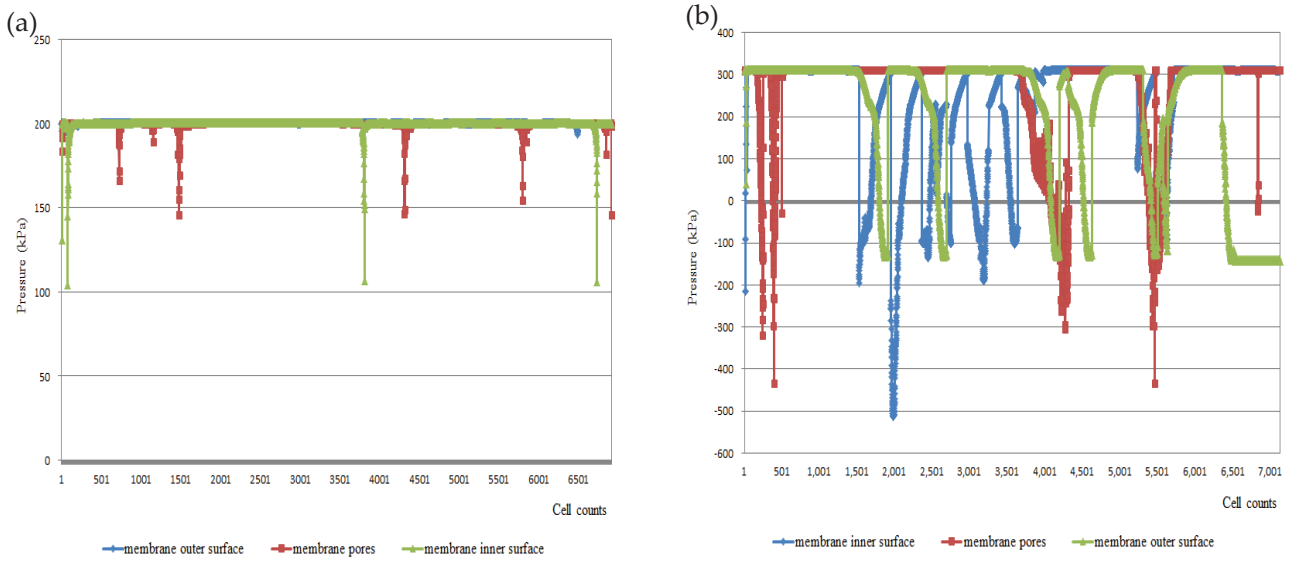

Fig. 6. Pressure profile at (a) backwashing on membrane and (b) channel washing on membrane.

Acknowledgment

This research was supported by a grant (18IFIP-C071145-06) and (18IFIP-B099786-05) from the Plant Research Program funded by the Ministry of Land, Infrastructure and Transport of the Korean Government.

References

[1] A.P.S. Yeo, A.W.K. Law, A.G. Fane, Factors affecting the performance of a submerged hollow fiber bundle, J. Membr. Sci., 280 (2006) 969–982.
[2] C. Albasi, Y. Bessiere, S. Desclaux, J.C. Remigy, Filtration of biological sludge by immersed hollow-fiber membranes: influence of initial permeability choice of operating conditions, Desalination, 146 (2002) 427–431.
[3] J. Busch, A. Cruse, W. Marquardt, Modeling submerged hollow-fiber membrane filtration for wastewater treatment, J. Membr. Sci., 288 (2007) 94–111.
[4] A.M. Wachinski, Membrane Processes for Water Reuse, McGraw Hill Companies, Inc., United States of America, 2013.
[5] K.V. Peinemann, S.P. Nunes, Membranes for Water Treatment, Wiley-VCH Verlag GmbH & Co. KGaA, United Kingdom, 2010.
[6] K.B. Lim, P.C. Wang, H. An, S.C.M. Yu, Computational studies for the design parameters of hollow fibre membrane modules, J. Membr. Sci., 529 (2017) 263–273.
[7] S. Veríssimo, K.-V. Peinemann, J. Bordado, New composite hollow fiber membrane for nanofiltration, Desalination, 184 (2005) 1–11.
[8] R. Ghidossi, J.V. Daurelle, D. Veyret, P. Moulin, Simplified CFD approach of a hollow fiber ultrafiltration system, Chem. Eng. J., 123 (2006) 117–125.
[9] N.C. Mat, Y. Lou, G.G. Lipscomb, Hollow fiber membrane modules, Curr. Opin. Chem. Eng., 4 (2014) 18–24.
[10] L. Zhuang, H. Guo, P. Wang, G. Dai, Study on the flux distribution in a dead-end outside-in hollow fiber membrane module, J. Membr. Sci., 495 (2015) 372–383.
[11] G.A. Fimbres-Weihs, D.E. Wiley, Review of 3D CFD modeling of flow and mass transfer in narrow spacer-filled channels in membrane modules, Chem. Eng. Process. Process Intensif., 49(7) (2010) 759–781.
[12] H. Yu, X. Yang, R. Wang, A.G. Fane, Numerical simulation of heat and mass transfer in direct membrane distillation in a hollow fiber module with laminar flow, J. Membr. Sci., 384 (2011) 107–116.
[13] X. Yang, H. Yu, R. Wang, A.G. Fane, Optimization of microstructured hollow fiber design for membrane distillation applications using CFD modeling, J. Membr. Sci., 421–422 (2012) 258–270.
[14] W. Ding, Application of CFD in Membrane Technique, Verfahrenstechnik Wassertechnik, Institute für Maschinenbau, Universität Duisburg Essen, Germany, 2012.
[15] S.H. Yoon, Inside-out and outside-in filtration modes in hollow fiber membrane process, 2016. Available at: http://onlinembr.info/inside-out-and-outside-in-filtration-modes-in-hollow-fiber-membrane-process/ (Assessed 09 January 2018).
[16] X. Guo, Y. Wang, H. Zhang, P. Li, C. Ma, Numerical and experimental investigation for cleaning process of submerged outside-in hollow fiber membrane, Water Sci. Technol., 76 (2017) 1283–1299.
[17] J.I. Oh, J.W. Choi, J.L. Lim, D.I. Kim, N.S. Park, A study on hydraulic modifications of low-pressure membrane inlet structure with CFD and PIV techniques, J. Korean Soc. Environ. Eng., 37 (2015) 607–618.
[18] O. Kavianipour, G.D. Ingram, H.B. Vuthaluru, Investigation into the effectiveness of feed spacer configurations for reverse osmosis membrane modules using Computational Fluid Dynamics, J. Membr. Sci., 526 (2017) 156–171.
[19] Taesung S&E, CFX Manual: Lecture 10 Turbulence: Introduction to ANSYS CFX, Taesung S&E, Korea, 2016. Available at: https://www.tsne.co.kr/ (Assessed 07 November 2017).